NANO LETTERS

pubs.acs.org/NanoLett

Letter

Single-Chirality Near-Infrared Carbon Nanotube Sub-Cellular Imaging and FRET Probes

Rachel Langenbacher, Januka Budhathoki-Uprety, Prakrit V. Jena, Daniel Roxbury, Jason Streit, Ming Zheng, and Daniel A. Heller*

Cite This: *Nano Lett.* 2021, 21, 6441−6448

Read Online

ACCESS | Metrics & More | Article Recommendations | Supporting Information

ABSTRACT: Applications of single-walled carbon nanotubes (SWCNTs) in bioimaging and biosensing have been limited by difficulties with isolating single-chirality nanotube preparations with desired functionalities. Unique optical properties, such as multiple narrow near-infrared bands and several modes of signal transduction, including solvatochromism and FRET, are ideal for live cell/organism imaging and sensing applications. However, internanotube FRET has not been investigated in biological contexts. We developed single-chirality subcellular SWCNT imaging probes and investigated their internanotube FRET capabilities in live cells. To functionalize SWCNTs, we replaced the surfactant coating of aqueous two-phase extraction-sorted single-chirality nanotubes with helical polycarbodiimide polymers containing different functionalities. We achieved single-chirality SWCNT targeting of different subcellular structures, including the nucleus, to enable multiplexed imaging. We also targeted purified (6,5) and (7,6) chiralities to the same structures and observed internanotube FRET within these organelles. This work portends the use of single-chirality carbon nanotube optical probes for applications in biomedical research.

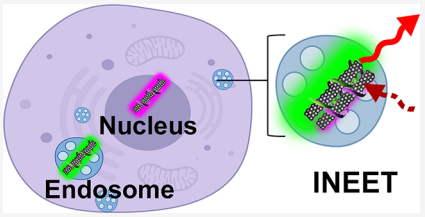

KEYWORDS: *Multiplexing, biosensor, dual-color imaging, near-infrared sensor, energy transfer*

INTRODUCTION

Semiconducting single-walled carbon nanotubes (SWCNTs) exhibit intrinsic, photostable, narrow-band near-infrared photoluminescence[1,2] that is of potential interest for use in bioanalytical probes and sensors.[3,4] To date, SWCNTs have been engineered for biomedical applications such as *in vivo* single-particle tracking,[5] to sense glucose *in vivo*,[6] to report dysregulated lipid accumulation in lysosomes,[7] to detect miRNA *in vivo*,[8] and to examine mechanisms of nuclear entry in cancer cells,[9] among others.[10]

The unique optical properties of carbon nanotubes confer several advantages over conventional fluorescent dyes. Typical fluorophores often photobleach easily, cannot be resolved as single molecules using conventional fluorescence microscopy, and have broad emission bands that limit multiplexing due to signal overlap.[11] Conversely, semiconducting SWCNTs are uniquely photostable and are produced with different structures of multiple chiral indices (n,m) which exhibit unique, narrow, and distinguishable emission bands. While the multiplexing of fluorescent dyes is often limited to 4−5 colors,[11] there are over 20 distinct SWCNT emitters; 17 distinct colors have been imaged simultaneously using hyperspectral imaging techniques.[12] Single nanotube emission is resolvable in tissues, cells, and intact animals; emission falls within the tissue-transparent window where absorbance, autofluorescence, and scattering are low, facilitating imaging in tissues *in vivo*.[13,14] Significant technical challenges have slowed the development of single-color/multiplexed SWCNT optical probes and sensors with desired functionalities, but the field is progressing steadily.

Carbon nanotubes have been derivatized with functional coatings for bioimaging and sensing applications. One set of examples, polycarbodiimides, synthetic helical polymers, have been shown to form noncovalent complexes with carbon nanotubes and can be used to effect modular derivatization to the nanotube surface.[15] Polycarbodiimides allow for control over surface charge, hydrophobicity, and the incorporation of multiple targeting moieties without direct/covalent modification of the nanotube structure. To date, these polymers have been used to control SWCNT energy transfer interactions, sensing, and localization in desired subcellular organelles, such as in cell nuclei.[9,16]

Förster resonance energy transfer (FRET) is a powerful tool in bioimaging. The development of SWCNT-based FRET probes offers certain advantages over traditional fluorophores.[15] Because their emission falls within the tissue-transparent NIR window, SWCNT-FRET probes could be detected at lower concentrations and at deeper imaging depths compared to other FRET approaches.[13,14] Individual SWCNTs

Received: March 22, 2021
Revised: June 29, 2021
Published: July 23, 2021

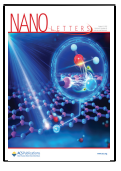

https://doi.org/10.1021/acs.nanolett.1c01093
Nano Lett. 2021, 21, 6441−6448

are distinguishable in cells, portending single-probe resolution capabilities.[13,14] FRET between nanotubes, also called internanotube exciton energy transfer (EET), has been demonstrated in solution[15] and in cells[17] using mixtures of SWCNT species.

As produced, SWCNTs exist as a heterogeneous mixture of many different chiralities.[12] A range of separation techniques have been developed, including density-gradient centrifugation,[18] column chromatography,[19] and aqueous two-phase extraction (ATPE).[20,21] The ATPE method is relatively scalable and can be used to separate a wide range of nanotube chiralities with high purity.[20] Like other separation techniques, ATPE is wrapping-dependent; ATPE currently requires either SWCNT suspension in surfactants or specific sequences of DNA.[22] The resulting single-chirality/color nanotubes from ATPE, or any other separation technique, must then be derivatized in order to confer solubility and biological functionalities. To functionalize separated nanotubes, attempts to remove the original surfactant/wrapping often result in irreversible aggregation; surfactant exchange procedures[25] have been most promising thus far.[23−26]

Herein, we developed single-chirality carbon nanotube-based optical probes to target subcellular locations to conduct multiplexed imaging in subcellular structures and to investigate internanotube FRET/EET in live cells. We developed a method to encapsulate ATPE-separated SWCNTs with synthetic polymers and found that these chirality-sorted nanotubes cloaked in polymers retained their desired functions, including eliciting nanotube−nanotube interactions to enable single-chirality, internanotube FRET/EET. These single-color nanotube complexes were used to investigate multiplexed imaging of specific subcellular structures in live cells, and it was found that these isolated chiralities could be targeted to different subcellular structures in the cell. Single-chirality probes were targeted separately to the cytosol and nucleus to validate a multiplexed imaging capability. We then investigated the potential for single-chirality internanotube FRET in live cells. Two separate chirality-enriched probes were targeted to the same location within cells by rewrapping them in oppositely charged helical polymers that elicited the same subcellular fate. We found that these polymer-SWCNT complexes facilitated internanotube FRET between the two probes in cytosolic compartments in live cells, portending the use of single-chirality carbon nanotube imaging and FRET probes for applications in biomedical research.

METHODS

ATPE Separation of SWCNTs. SWCNTs were dispersed using surfactants, and individual chiralities were separated using the aqueous two-phase extraction method described by Fagan et al.[20,21] Reagents were as follows: SWCNT powder (Sigma-Aldrich Carbon nanotube, single-walled (6,5) chirality >95% >93% carbon as SWCNT 0.7−0.9 nm diameter or Carbon nanotube, single-walled (7,6) chirality >77% carbon as SWCNT 0.7−1.1 nm diameter), sodium cholate hydrate (SC, Sigma-Aldrich from ox and/or sheep ≥99%), sodium dodecyl sulfate (SDS, Sigma-Aldrich ACS Reagent ≥99%), sodium deoxycholate (DOC, Sigma-Aldrich ≥99%) polyethylene glycol (PEG, Sigma-Aldrich Bioultra mw: 6000 Da), and dextran (Sigma-Aldrich from *Leuconostoc mesenteroides*, mw: 64 000−76 000 Da). Briefly, 1 mg of dry nanotubes was added to a 1.0 mL solution of aqueous 2% w/w SC and sonicated (750 W, 20 kHz, 40% amplitude, SONICS Vibracell) at low temperature for 40 min using a CoolRack M30 PF (BioCision) stored at −20 °C prior to use. To remove carbon nanotube aggregates, amorphous carbon, and residual catalyst, ultracentrifugation was performed at 280,000 g for 30 min, after which the top 75% of the solution was collected for subsequent ATPE separations, while the bottom 25% was discarded. ATPE separations were carried out at room temperature, at polymer concentrations of approximately 8% PEG and 9% dextran. Further ATPE details are included in Figures S1−S2 and Table S1. A benchtop centrifuge (Fisher-Scientific Sprout model, Heathrow Scientific) was used to accelerate phase separation, and separations were monitored using UV−vis−NIR spectroscopy acquired with a JASCO V-670 spectrophotometer.

Wrapping Exchange and Characterization of Re-wrapped SWCNTs. The polycarbodiimide polymers used in this study were previously synthesized and characterized as reported.[9,15,16,27] Chirality-enriched nanotubes from the aforementioned ATPE separation suspended in a 0.1% (w/w) DOC solution were filtered to remove surfactant using a 10 kDa centrifugal filter (Amicon Ultracel, Merk Milipore Ltd.) in the presence of 2% (w/w) dextran (MW 64 000−76 000 Da) to prevent aggregation; washes were performed with PBS. Removal of surfactant was monitored via shifts in UV−vis−NIR absorbance using a JASCO V-670 spectrophotometer. For the (6,5) nanotube, the absorbance peak at 1000 nm was monitored, and for the (7,6) nanotube, the absorbance peak at 1130 nm was used. After the first wash step, 30 μL of the aqueous amine-functionalized polycarbodiimide polymer (4 mg in 1.0 mL water stock solution) were added to the residue of (6,5) SWCNTs. After surfactant was removed via five additional wash steps and confirmed via red-shifting of the UV−vis-NIR absorbance peak, the (6,5) SWCNTs were resuspended in PBS and probe-tip sonicated (20% amplitude, SONICS Vibracell) at low temperature for 10 min using a CoolRack M30 PF (BioCision) stored at −20 °C prior to use. Unassociated polymer was removed using centrifugal filtration (Millipore Amicon, 100 kDa). This same procedure was also used to resuspend (7,6) SWCNTs with the carboxy-functionalized polymer ((7,6) carboxy-poly SWCNTs), and a second preparation of (6,5) SWCNTs with guanidinium-functionalized polymer ((6,5) guanidinium-poly SWCNTs). Ultrapure water (18.2 mΩ) was used for all washes and aqueous suspensions.

Cell Culture. Cells were purchased from the American Type Culture Collection (ATCC), and reagents were obtained from Gibco Life technologies.

HeLa cells were cultured in DMEM supplemented with 10% (v/v) heat-inactivated FBS, 1% penicillin streptomycin, 1% glutamine, and 2.5% HEPES at 37 °C in humidified air containing 5% CO_2. Cells were trypsinized, washed, and plated into 35 mm glass-bottom dishes (MatTek) and used after 24 h at ∼80% confluence. Polymer-wrapped nanotubes were diluted in DI H_2O and added to cell dishes to a concentration of 0.2 mg/L. The cells were incubated with nanotubes for 1 h, after which the cells were washed with PBS three times and fresh medium was added. Cells were then imaged 24 h after this wash step.

RAW 264.7 cells were cultured in DMEM supplemented with 10% (v/v) heat-inactivated FBS, 1% penicillin streptomycin, 1% glutamine, and 2.5% HEPES at 37 °C in humidified air containing 5% CO_2. Cells were scraped, washed, and plated in 35 mm glass-bottom dishes (MatTek) and used after 24 h at ∼80% confluence. Cells were preincubated in serum-free

https://doi.org/10.1021/acs.nanolett.1c01093
Nano Lett. 2021, 21, 6441−6448

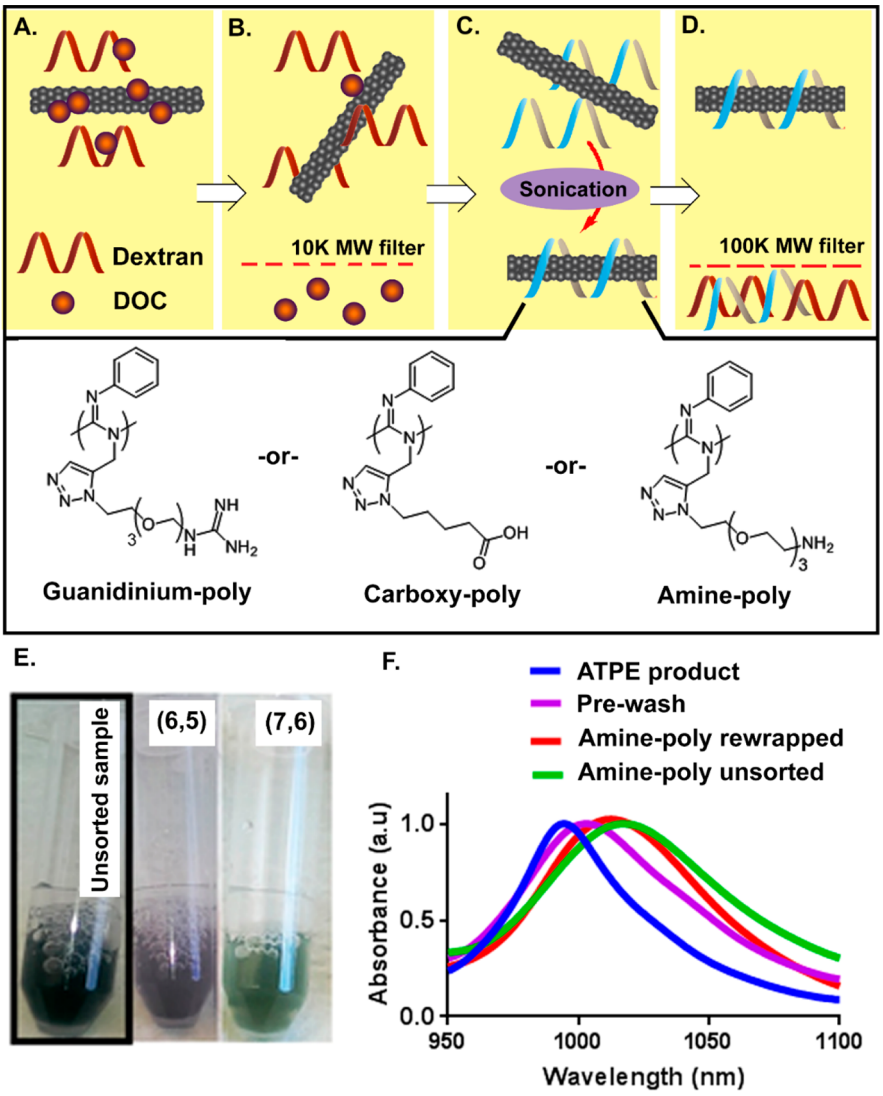

Figure 1. Rewrapping protocol. (A) Schematic showing ATPE enriched nanotubes suspended in 0.1% DOC (orange circles). Dextran was added to a concentration of 2% w/w (red). (B) Centrifugal filtration (10 kDa MWCO) was carried out to remove surfactant. After the second wash step, the desired polycarbodiimide wrapping (blue) was added. (C) Probe tip sonication was performed. (D) Dextran was removed using 100 kDa MWCO centrifugal filter. The residue was resuspended in DI H_2O. (E) Images of unsorted sample and rewrapped, ATPE-sorted samples of (6,5) and (7,6) nanotube species. (F) Absorbance spectra of ATPE product in 0.1% DOC (blue); sorted nanotubes after one wash prior to polycarbodiimide addition (magenta); ATPE sorted, amine-poly rewrapped nanotubes (red); and unsorted, amine-poly wrapped nanotubes (green).

media for 12 h. Then, polymer-wrapped nanotubes were diluted in DI water and added to dishes. Control dishes were treated with 1 mg/L of either (6,5) amine-poly SWCNT or (7,6) carboxy-poly SWCNT, incubated for 24 h prior to imaging. For examination of (6,5) amine-poly SWCNTs and (7,6) carboxy-poly SWCNTs interactions within cells, dishes were incubated with 1 mg/L (6,5) amine-poly SWCNT for 1 h and washed. These cells were then incubated for 3 h, treated with 1 mg/L (7,6) carboxy-poly SWCNTs for 12 h, washed, and used for imaging studies. Concentrations were estimated as described for stock solutions and diluted from stock solutions for each titration.

Live Cell near-Infrared Imaging and near-Infrared Hyperspectral Microscopy. The near-infrared photoluminescence imaging and spectroscopy of cell probes were performed using a near-infrared hyperspectral microscope. Briefly, this system is comprised of a continuous wave 730 nm diode laser (output power 2W), homogenized via a custom-built beam shaper to ensure even illumination across the field of view. A long pass dichroic mirror (cut-on wavelength 875 nm; Semrock) was used to reflect the light source to the Olympus IX-71 microscope (with custom modifications for transmission in the 900−1400 nm optical window), and emission was collected using a 2D InGaAs array (Photon Etc.). Broad-band images were obtained under white light conditions and after 730 nm excitation (0.2 s exposure) as previously reported.[9,15] Hyperspectral "cubes" were obtained as previously reported.[9,15] Data were then processed using ImageJ software (NIH) and custom Matlab codes to subtract background and correct for artifacts such as dead pixels and slight aberrations in the excitation profile. To obtain spectrally defined images from selected wavelength ranges (i.e., 976 nm−1028 nm and 1124 nm−1176 nm), ImageJ software was used to construct a single composite image from the 4 nm binned images composing each hyperspectral cube over the selected range. Photoluminescence excitation/emission plots were

https://doi.org/10.1021/acs.nanolett.1c01093
Nano Lett. 2021, 21, 6441−6448

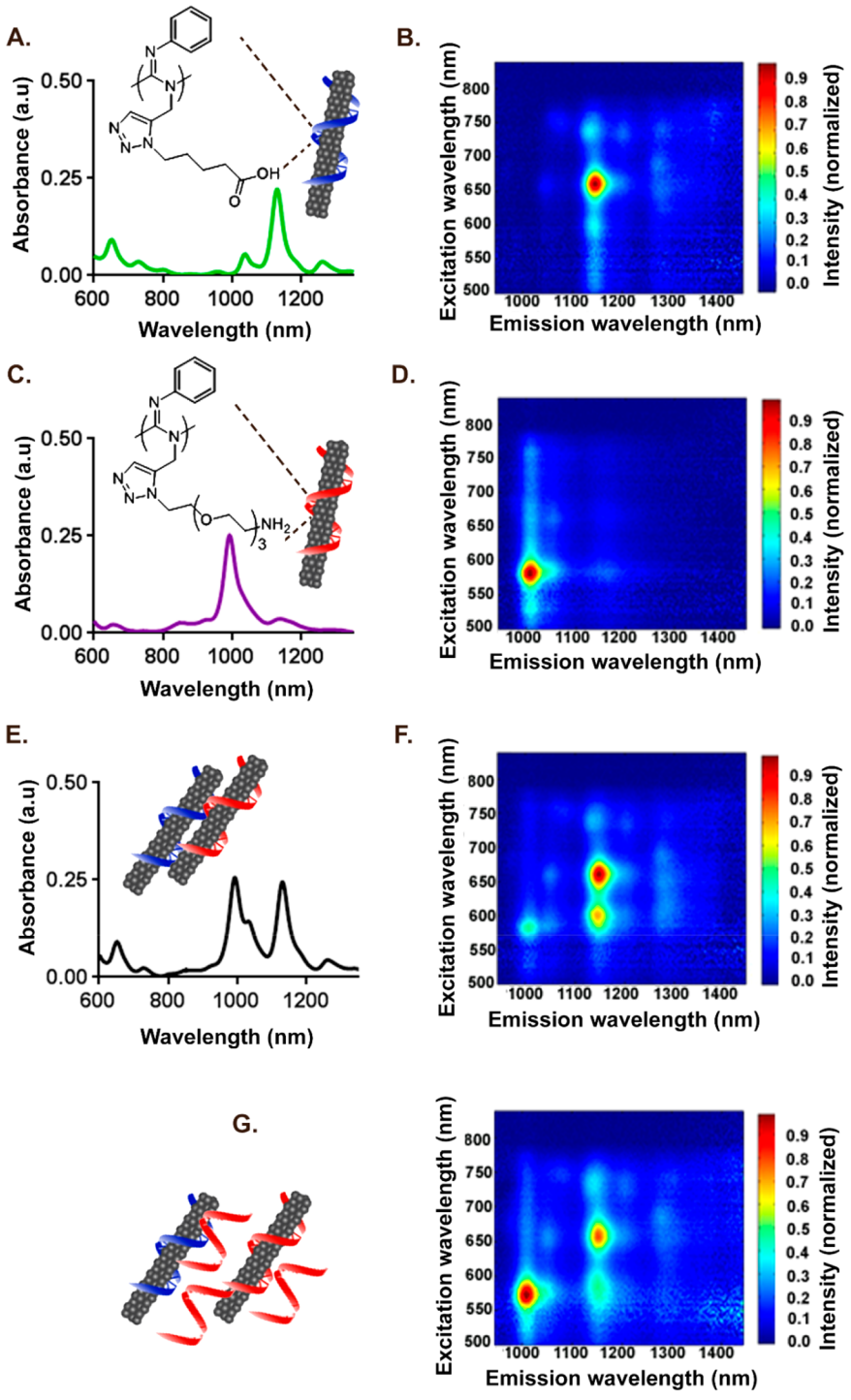

Figure 2. Energy transfer between purified SWCNT chiralities. (A) UV−vis-NIR absorbance spectrum and (B) Photoluminescence plot of (7,6) carboxy-poly SWCNTs in PBS. (C) UV−vis−NIR absorbance spectrum and (D) photoluminescence plot of (6,5) amine-poly SWCNTs in PBS. (E) UV−vis−NIR spectrum and (F) photoluminescence plot of mixture of (6,5) amine-poly SWCNTs and (7,6) carboxy-poly SWCNTs in PBS. (G) Photoluminescence plot of mixture, with excess free amine-poly added. Intensities of photoluminescence plots and absorbance of UV−vis−NIR spectra were self-normalized.

obtained as previously described.[8] For all experiments, measurements were obtained in triplicate across three wells.

Statistical Analysis. Graphpad Prism version 7 was used for all statistical analyses. Statistical significance was analyzed using ANOVA testing. $p < 0.05$ was used as a cutoff for significance.

RESULTS AND DISCUSSION

Wrapping Exchange. We replaced surfactant from ATPE chirality-enriched, surfactant-suspended nanotubes, postpurification, with polycarbodiimide polymers functionalized with carboxylic acid, amine, or guanidinium substituents (carboxy-poly, amine-poly, and guanidinium-poly respectively). We sought to first remove the surfactant through repeated wash

https://doi.org/10.1021/acs.nanolett.1c01093
Nano Lett. 2021, 21, 6441−6448

steps via centrifugal filtration without aggregation. High molecular weight dextran (MW: 64 000−76 000 Da) was introduced during wash steps to prevent aggregation. Figure 1A−D illustrate this approach. We then used brief probe tip sonication of the mixture in the presence of the desired polycarbodiimide polymer to redisperse the suspension (Figure 1E).

We monitored the rewrapping progress using absorbance spectroscopy, monitoring the peak broadening and red-shifting, characteristic of surfactant removal from the nanotube surface, arising from increased heterogeneity of surface coverage and exposed surface area allowing increased interaction of the nanotube surface with water.[17] Absorbance spectra were taken of ATPE product, prewash product (after a single centrifugal filter step), and amine-poly rewrapped (ATPE product after rewrapping with amine-poly), shown in Figure 1F. The wash steps and introduction of the polycarbodiimide with probe tip sonication corresponded with broadening and red-shifting relative to surfactant-only suspended nanotubes, with the center wavelength corresponding to that of unsorted, amine-poly wrapped nanotubes. These shifts were seen in both nanotubes rewrapped in negatively charged polymers and nanotubes rewrapped in positively charged polymers, and representative spectra of amine-poly and carboxy-poly rewrapping are shown in Figure S2. Additionally, photoluminescent plots showed emission wavelength shifts in rewrapped samples compared to ATPE products (Figure S5). This broadening and red-shifting, consistent with surfactant removal from the nanotube surface,[18] suggest the successful exchange of surfactant for polycarbodiimide on the chirality-enriched nanotube suspensions.

Spectral Effects of Surface Charge Interactions. We examined FRET between ATPE-sorted, polymer-encapsulated nanotube species. Previously, we found that polycarbodiimide polymers can be used to modulate SWCNT surface charge to either positive or negative zeta potential values.[15] Coulombic forces between the primary amine groups (cationic protonated form) and the carboxylic acid groups (anionic carboxylate form) facilitated aggregation of amine-poly SWCNTs and carboxy-poly SWCNTs, resulting in EET/FRET.[15] Herein, we wrapped the sorted (7,6) nanotube species in a carboxylic acid functionalized polycarbodiimide ((7,6) carboxy-poly SWCNT) and the (6,5) SWCNT with the primary amine-functionalized polycarbodiimide ((6,5) amine-poly SWCNT) (Figure 2A, C, E). The photoluminescence of rewrapped, chirality enriched (6,5) amine-poly SWCNTs and (7,6) carboxy-poly SWCNTs showed strong emission corresponding to their E_{11} bands (Figure 2 B, D). In the mixed sample (Figure 2F), we observed the relative decrease of the (6,5) SWCNT emission intensity and increase in (7,6) species intensity. We also observed the appearance of a peak at approximately 575 nm excitation and 1140 nm emission. This band most probably corresponds to the (8,4) chirality which likely was not completely removed during the purification process but was not present in an optically significant concentration until energy transfer caused its emission intensity to increase substantially. The addition of free amine-poly to this mixed sample to disrupt charge−charge interactions between (6,5) amine-poly SWCNTs and (7,6) carboxy-poly SWCNTs resulted in a relative attenuation in the intensity of this peak and the (7,6) peak, and a corresponding relative increase in the (6,5) peak intensity (Figure 2G). These results suggest energy transfer between the enriched samples of (7,6) carboxy-poly SWCNTs and (6,5) amine-poly SWCNTs.

Two-Color Imaging of Subcellular Structures. We next sought to evaluate the potential of the ATPE-sorted, polymer encapsulated nanotube complexes for multiplexed live cell imaging of subcellular structures. Previously, we observed that unsorted guanidinium-poly SWCNTs localize to the nucleus of HeLa cells, and amine-poly SWCNTs nanotubes remain in the cytosolic region.[9] We treated HeLa cells with (6,5)-guanidinium-poly SWCNTs, incubated for 1 h, washed, and then treated with (7,6) amine-poly SWCNTs. We conducted near-infrared hyperspectral microscopy after 24 h to collect both near-infrared broadband images and spectrally defined images (Figures 3A−D, S3). In the broad-band near-infrared

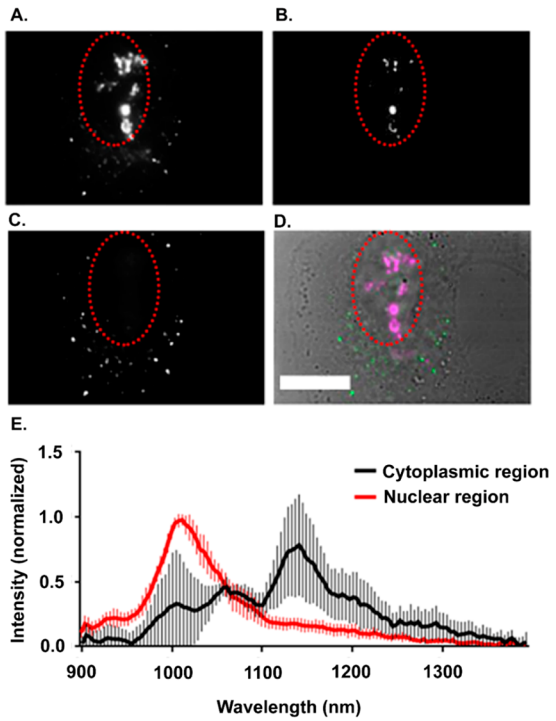

Figure 3. Subcellular localization of single-color probes in live cells. (A) Representative images of broadband NIR emission of HeLa cells treated with (6,5) guanidinium-poly SWCNTs and (7,6) amine-poly SWCNTs, (B) 975−1025 nm NIR emission, (C) 1125−1175 nm NIR emission, and (D) overlay of 975−1025 nm emission (magenta), 1125−1175 nm emission (green), and brightfield image. Nuclear region shown with red dotted line. Scale bar = 20 μm. (E) Averaged emission spectra from the apparent nuclear (n = 13 ROIs) and cytoplasmic regions (n = 15 ROIs) of the representative image shown. Of (6,5) guanidinium-poly SWCNTs (n = 123 ROIs), 76% (Stdev = 9%) were found in the nuclear region and 98% (Stdev = 2%) of (7,6) amine-poly SWCNTs were found in the cytosolic region. Three technical replicates were measured.

images, we observed nanotube emission in both the cytosolic and nuclear regions of the cells. The spectrally resolved images showed differential distribution of the two nanotube probes. Emission at 976 nm−1028 nm, corresponding to the (6,5) E_{11} emission, localized primarily to the nuclear region of the cells (Figure 3B), and emission at 1124 nm−1176 nm, corresponding to the (7,6) E_{11} band, localized primarily to the cytosolic region (Figure 3C). Averaged emission spectra were consistent with this pattern (Figure 3E). Cells treated with (6,5) amine-poly SWCNTs and (7,6) amine-poly SWCNTs did not show

https://doi.org/10.1021/acs.nanolett.1c01093
Nano Lett. 2021, 21, 6441−6448

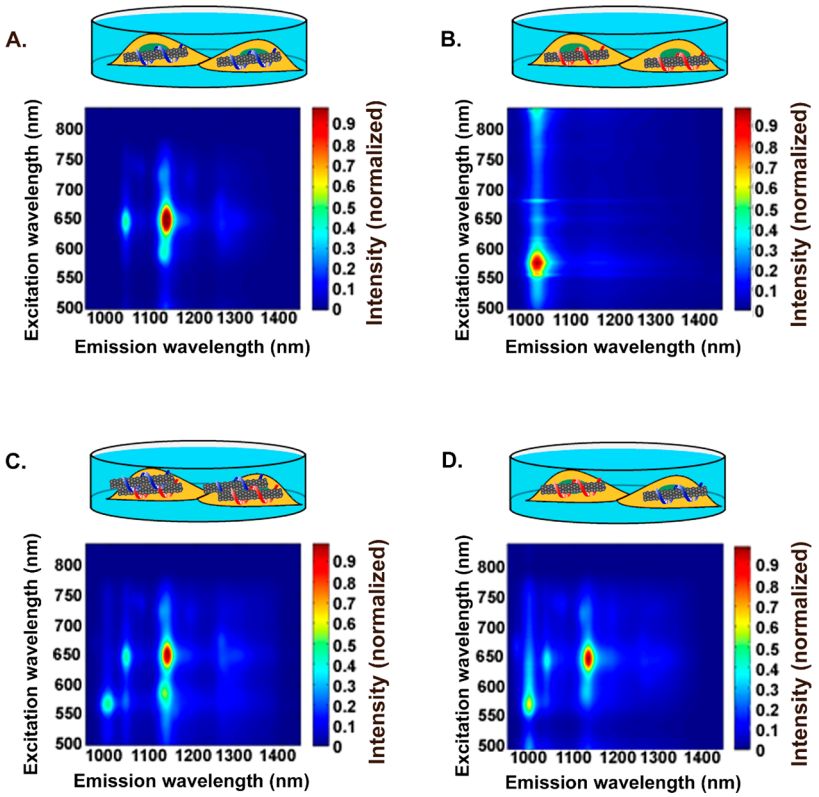

Figure 4. Internanotube exciton energy transfer in live cells. (A) Photoluminescence plot of cells treated with (7,6) carboxy-poly SWCNTs alone (images above spectra are cartoons depicting the experimental condition). (B) Photoluminescence plot of cells treated with (6,5) amine-poly SWCNTs alone. (C) Photoluminescence plot of cells treated with both (6,5) amine-poly SWCNTs and (7,6) carboxy-poly SWCNTs. (D) Photoluminescence plot of mixture of two cell populations treated separately with either (6,5) amine-poly SWCNTs or (7,6) carboxy-poly SWCNTs. Plots are representative single readings and are normalized to themselves. Diagrams are representative; nanotubes are not drawn to scale.

this distribution pattern; under these conditions both SWCNT species were detected at significant levels only in the cytosolic region (Figure S4).

Internanotube Energy Transfer within Subcellular Structures. We investigated internanotube FRET between single-color probes within live cells using polymer-SWCNT complexes of opposite electrostatic charges to target the same organelles. Previously we found that both amine- and carboxy-polymer wrapped SWCNTs entered cells via endocytosis and colocalized within the same subcellular locations.[16] We thus used these polymers to study intracellular EET between the (7,6) and (6,5) nanotubes. RAW 264.7 macrophages (used for their increased rate of endocytosis) were treated with (6,5) amine-poly SWCNTs alone, (7,6) carboxy-poly SWCNTs alone, and a mixture of both. In addition, the probes were separately administered to two cell populations that were then mixed after incubation and wash steps to prevent nanotube–nanotube interactions within the cells.

Near-infrared photoluminescence excitation/emission spectroscopy was conducted on the live cells. The resulting spectra showed characteristic E_{11} bands of the (6,5) (Figure 4 A) and (7,5) (Figure 4 B) chiralities in cells treated separately with the polymer-SWCNT complexes. In cells treated with both (6,5) amine-poly SWCNTs and (7,6) carboxy-poly SWCNTs, we observed a relative increase in the emission of the (7,6) species and a concomitant relative decrease of the (6,5) emission band (Figure 4 C). We observed the appearance of a peak at approximately 575 nm excitation and 1140 nm emission. As in our investigation of internanotube FRET in solution, this band most probably corresponds to the (8,4) chirality which likely was not completely removed during the purification process but was not present in a significant concentration until energy transfer caused its emission intensity to increase and become evident. In the sample where two separate cell populations were treated individually with single-color probes, where the cells were then combined, we saw essentially the combination of the spectral features from the two individual samples with no significant additional spectral features, including the peak attributed to the (8,4) chirality (Figure 4 D). Also, the relative intensity of the (6,5) band was greater than in the mixed sample. These results suggest significant energy transfer between the SWCNTs in cells treated with both probes, as compared to the other conditions.

CONCLUSIONS

This work makes new headway toward the development of separated, single-color carbon nanotube species for live cell imaging and FRET-based sensor applications, presenting a method for isolating and constructing single-color probes. We report the development and application of single-chirality enriched, multiplexed and targeted carbon nanotube probes through a wrapping exchange protocol for ATPE-sorted single-walled carbon nanotubes to enable encapsulation with a synthetic polymer. We then demonstrated that rewrapped nanotube complexes, constructed using oppositely charged encapsulating polymers encapsulating distinct, separated nanotube chiralities, exhibited internanotube energy transfer between the small and large band gap chiralities. Additionally,

https://doi.org/10.1021/acs.nanolett.1c01093
Nano Lett. 2021, 21, 6441−6448

we report that these separated, polymer-encapsulated nanotubes can be targeted to specific subcellular compartments, resulting in multiplexed cellular imaging. Finally, using the encapsulating polymer to simultaneously control subcellular targeting and internanotube interactions, we found that energy transfer between sorted SWCNTs could be resolved within live cells, and energy transfer was only observed when colocalization to the same subcellular compartment occurred.

Although an increasing library of materials can be used to facilitate the isolation of SWCNTs,[24−26,28,29] this work demonstrates that sorted SWCNT chiralities, originally encapsulated by one set of materials, can then be rewrapped with moieties that confer desired subcellular-targeting behavior. Regarding the resulting FRET probes, we believe that similar materials could be engineered to serve as reporters of molecular interactions in specific cellular compartments. Because approximately 20 photoluminescent, structurally distinct SWCNTs are available, can be resolved at the single-nanotube level, and have bright, nonphotobleachable emission that falls within the tissue transparent NIR window, we believe that SWCNT-based FRET probes will be of interest for multiplexed bioimaging and sensing applications in live cells and animals.

■ ASSOCIATED CONTENT

Supporting Information

The Supporting Information is available free of charge at https://pubs.acs.org/doi/10.1021/acs.nanolett.1c01093.

Additional information about ATPE separation of nanotubes and spectral characterization, additional imaging data (PDF)

■ AUTHOR INFORMATION

Corresponding Author

Daniel A. Heller − *Weill Cornell Medical College, New York, New York 10065, United States; Memorial Sloan Kettering Cancer Center, New York, New York 10065, United States;* orcid.org/0000-0002-6866-0000; Email: hellerd@mskcc.org

Authors

Rachel Langenbacher − *Weill Cornell Medical College, New York, New York 10065, United States;* orcid.org/0000-0002-5284-3566

Januka Budhathoki-Uprety − *Department of Textile Engineering, Chemistry, and Science, North Carolina State University, Raleigh, North Carolina 27695, United States;* orcid.org/0000-0003-3395-4823

Prakrit V. Jena − *Memorial Sloan Kettering Cancer Center, New York, New York 10065, United States;* orcid.org/0000-0001-5493-3058

Daniel Roxbury − *Department of Chemical Engineering, University of Rhode Island, Kingston, Rhode Island 02881, United States;* orcid.org/0000-0003-2812-3523

Jason Streit − *Air Force Research Laboratory, Wright-Patterson Air Force Base, Ohio 45433, United States;* orcid.org/0000-0003-3209-2141

Ming Zheng − *National Institute of Standards and Technology, Gaithersburg, Maryland 20089, United States;* orcid.org/0000-0002-8058-1348

Complete contact information is available at: https://pubs.acs.org/10.1021/acs.nanolett.1c01093

Notes

The authors declare the following competing financial interest(s): D.H. is a cofounder and officer with equity interest of Goldilocks Therapeutics Inc., LipidSense Inc., and Nirova Biosense Inc., as well as a member of the scientific advisory board of Concarlo Holdings LLC, Nanorobotics Inc., and Mediphage Bioceuticals, Inc.

■ ACKNOWLEDGMENTS

This work was supported in part by the NIH New Innovator Award (DP2-HD075698), the Cancer Center Support Grant (P30-CA008748), the National Science Foundation CAREER Award (1752506), the American Cancer Society Research Scholar Grant (GC230452), the Pershing Square Sohn Cancer Research Alliance, the Honorable Tina Brozman Foundation for Ovarian Cancer Research, the Expect Miracles Foundation - Financial Services Against Cancer, the Anna Fuller Fund, the Louis V. Gerstner Jr. Young Investigator's Fund, the Frank A. Howard Scholars Program, MSK's Cycle for Survival's Equinox Innovation Award in Rare Cancers, the Alan and Sandra Gerry Metastasis Research Initiative, Mr. William H. Goodwin and Mrs. Alice Goodwin and the Commonwealth Foundation for Cancer Research, the Experimental Therapeutics Center, the Imaging & Radiation Sciences Program, and the Center for Molecular Imaging and Nanotechnology of Memorial Sloan Kettering Cancer. R.L. was supported by an NIH T32 training grant (T32-GM73546-9). D.R. was supported by the American Cancer Society Roaring Fork Valley Postdoctoral Fellowship (PF-13-388801-TBG) as well as a National Science Foundation CAREER Award (1844536), J.B. was supported by the Tow Foundation Postdoctoral Fellowship, Center for Molecular Imaging and Nanotechnology at MSKCC, P.V.J. was supported by an NIH NCI T-32 fellowship (2T32CA-062948-21).

■ REFERENCES

(1) Hong, G.; Diao, S.; Antaris, A. L.; Dai, H. Carbon Nanomaterials for Biological Imaging and Nanomedicinal Therapy. *Chem. Rev.* **2015**, *115*, 10816−10906.

(2) Jena, P. V.; Galassi, T. V.; Roxbury, D.; Heller, D. a. Review—Progress toward Applications of Carbon Nanotube Photoluminescence. *ECS J. Solid State Sci. Technol.* **2017**, *6*, M3075−M3077.

(3) Williams, R. M.; Chen, S.; Langenbacher, R. E.; Galassi, T. V.; Harvey, J. D.; Jena, P. V.; Budhathoki-Uprety, J.; Luo, M.; Heller, D. A. Harnessing nanotechnology to expand the toolbox of chemical biology. *Nat. Chem. Biol.* **2021**, *17* (2), 129−137.

(4) Jena, P. V.; Galassi, T. V.; Roxbury, D.; Heller, D. A. Progress toward applications of carbon nanotube photoluminescence. *ECS J. Solid State Sci. Technol.* **2017**, *6* (6), M3075.

(5) Gao, Z.; Danné, N.; Godin, A.; Lounis, B.; Cognet, L. Evaluation of Different Single-Walled Carbon Nanotube Surface Coatings for Single-Particle Tracking Applications in Biological Environments. *Nanomaterials* **2017**, *7*, 393.

(6) Barone, P. W.; Parker, R. S.; Strano, M. S. In vivo fluorescence detection of glucose using a single-walled carbon nanotube optical sensor: Design, fluorophore properties, advantages, and disadvantages. *Anal. Chem.* **2005**, *77*, 7556−7562.

(7) Jena, P. V.; et al. A Carbon Nanotube Optical Reporter Maps Endolysosomal Lipid Flux. *ACS Nano* **2017**, *11*, 10689−10703.

(8) Harvey, J. D.; Jena, P. V.; Baker, H. A.; Zerze, G. H.; Williams, R. M.; Galassi, T. V.; Roxbury, D.; Mittal, J.; Heller, D. A. A carbon nanotube reporter of microRNA hybridization events in vivo. *Nature biomedical engineering 1.4* **2017**, *1*, 0041.

(9) Budhathoki-Uprety, J.; Langenbacher, R. E.; Jena, P. V.; Roxbury, D.; Heller, D. A. Carbon Nanotube Optical Sensor Reports

Nuclear Entry via a Noncanonical Pathway. *ACS Nano* **2017**, *11*, 3875−3882.
(10) Mundra, R. V.; Wu, X.; Sauer, J.; Dordick, J. S.; Kane, R. S. Nanotubes in biological applications. *Curr. Opin. Biotechnol.* **2014**, *28*, 25−32.
(11) Resch-Genger, U.; Grabolle, M.; Cavaliere-Jaricot, S.; Nitschke, R.; Nann, T. Quantum dots versus organic dyes as fluorescent labels. *Nat. Methods* **2008**, *5*, 763−775.
(12) Roxbury, D.; Jena, P. V.; Williams, R. M.; Enyedi, B.; Niethammer, P.; Marcet, S.; Verhaegen, M.; Blais-Ouellette, S.; Heller, D. A. Hyperspectral Microscopy of Near-Infrared Fluorescence Enables 17-Chirality Carbon Nanotube Imaging. *Sci. Rep.* **2015**, *5*, 1−6.
(13) Bachilo, S. M.; Strano, M. S.; Kittrell, C.; Hauge, R. H.; Smalley, R. E.; Weisman, R. B. Structure-assigned optical spectra of single-walled carbon nanotubes. *Science* **2002**, *298*, 2361−2366.
(14) Hong, G.; Diao, S.; Antaris, A. L.; Dai, H. Carbon Nanomaterials for Biological Imaging and Nanomedicinal Therapy. *Chem. Rev.* **2015**, *115*, 10816−10906.
(15) Budhathoki-Uprety, J.; Jena, P. V.; Roxbury, D.; Heller, D. a. Helical polycarbodiimide cloaking of carbon nanotubes enables inter-nanotube exciton energy transfer modulation. *J. Am. Chem. Soc.* **2014**, *136*, 15545−15550.
(16) Budhathoki-Uprety, J.; Harvey, J. D.; Isaac, E.; Williams, R. M.; Galassi, T. V.; Langenbacher, R. E.; Heller, D. A. Polymer cloaking modulates the carbon nanotube protein corona and delivery into cancer cells. *J. Mater. Chem. B* **2017**, *5* (32), 6637−6644.
(17) Gravely, M.; Daniel, R. Multispectral Fingerprinting Resolves Dynamics of Nanomaterial Trafficking in Primary Endothelial Cells. *bioRxiv* **2020**.
(18) Arnold, M. S.; Green, A. a.; Hulvat, J. F.; Stupp, S. I.; Hersam, M. C. Sorting carbon nanotubes by electronic structure using density differentiation. *Nat. Nanotechnol.* **2006**, *1*, 60−65.
(19) Liu, H.; Tanaka, T.; Kataura, H. Optical isomer separation of single-chirality carbon nanotubes using gel column chromatography. *Nano Lett.* **2014**, *14*, 6237−6243.
(20) Fagan, J. A.; Khripin, C. Y.; Silvera Batista, C. A.; Simpson, J. R.; Hároz, E. H.; Hight Walker, A. R.; Zheng, M. Isolation of specific small-diameter single-wall carbon nanotube species via aqueous two-phase extraction. *Adv. Mater.* **2014**, *26*, 2800−2804.
(21) Fagan, J. A.; Hároz, E. H.; Ihly, R.; Gui, H.; Blackburn, J. L.; Simpson, J. R.; Lam, S.; Hight Walker, A. R.; Doorn, S. K.; Zheng, M. Isolation of > 1 nm Diameter Single-Wall Carbon Nanotube Species Using Aqueous Two-Phase Extraction. *ACS Nano* **2015**, *9*, 5377−5390.
(22) Dong, L.; Joseph, K. L.; Witkowski, C. M.; Craig, M. M. Cytotoxicity of single-walled carbon nanotubes suspended in various surfactants. *Nanotechnology* **2008**, *19*, 255702.
(23) Streit, J. K.; Fagan, J. a.; Zheng, M. A Low Energy Route to DNA-Wrapped Carbon Nanotubes via Replacement of Bile Salt Surfactants. *Anal. Chem.* **2017**, *89*, 10496−10503.
(24) Nißler, R.; Mann, F. A.; Preiß, H.; Selvaggio, G.; Herrmann, N.; Kruss, S. Chirality enriched carbon nanotubes with tunable wrapping: Via corona phase exchange purification (CPEP). *Nanoscale* **2019**, *11*, 11159−11166.
(25) Nißler, R.; Kurth, L.; Li, H.; Spreinat, A.; Kuhlemann, I.; Flavel, B. S.; Kruss, S. Sensing with chirality pure near infrared fluorescent carbon nanotubes. *ChemRxiv* **2020**, 44−47.
(26) Chen, F.; Wang, B.; Chen, Y.; Li, L. J. Toward the extraction of single species of single-walled carbon nanotubes using fluorene-based polymers. *Nano Lett.* **2007**, *7*, 3013−3017.
(27) Budhathoki-Uprety, J.; Novak, B. M. Synthesis of alkyne-functionalized helical polycarbodiimides and their ligation to small molecules using 'click' and Sonogashira reactions. *Macromolecules* **2011**, *44*, 5947−5954.
(28) Ao, G.; Zheng, M. Preparation and separation of DNA-wrapped carbon nanotubes. *Curr. Protoc. Chem. Biol.* **2015**, *7*, 43−51.
(29) Welsher, K.; Liu, Z.; Sherlock, S. P.; Robinson, J. T.; Chen, Z.; Daranciang, D.; Dai, H. A route to brightly fluorescent carbon nanotubes for near-infrared imaging in mice. *Nat. Nanotechnol.* **2009**, *4* (11), 773.

https://doi.org/10.1021/acs.nanolett.1c01093
Nano Lett. 2021, 21, 6441−6448